

变深度螺旋槽止推轴承的边界元法计算*

朱 勤 谢友柏 虞 烈 薛永宽
(西安交通大学润滑理论及轴承研究所, 西安 710049)

摘 要 本文以分析变深度螺旋槽止推轴承为例介绍了边界元法在润滑力学研究领域中应用,以及相应的边界条件的处理方法,同时还讨论了轴承的尺寸参数对其性能参数的影响。

关键词 螺旋槽, 止推轴承, 边界元法, 润滑力学

1. 前 言

本世纪七十年代以后,螺旋槽轴承越来越受到人们的重视^[1,2]。近年来,由于采用“翼栅理论”^[3]和边界元法^[4]已经建立起比较完整的计算等深度螺旋槽轴承性能的二维理论,螺旋槽轴承便以其突出的优点^[5]而在高速旋转机械中得到了广泛的应用^[6-8]。本文报道运用具有代数方程组数少、输入数据少、计算时间短及精度高等优点^[9]的边界元法对变深度螺旋槽止推轴承的计算结果。

2. 基 本 公 式

图 1(a)所示为变深度螺旋槽止推轴承。螺旋槽曲线为:

$$\rho = r_1 e^{c_1 \theta \beta \cdot \theta}$$

式中: β 为螺旋角。螺旋槽数目为 K 。根据周期性条件取其中的 $1/K$ 即一块瓦来分析如图 1(b)所示。止推平面包含的区域 Ω_1 系由边界 I、II、III、IV 和 V 组成,其所满足的雷诺方程为:

$$\nabla^2 P = \frac{\partial^2 P}{\partial x^2} + \frac{\partial^2 P}{\partial y^2} = 0 \quad (1)$$

槽所包含的区域 Ω_2 系由边界 I' 和 II' 组成,其所满足的雷诺方程为:

$$\frac{\partial}{\partial x} \left(\frac{h^3}{\mu} \frac{\partial P}{\partial x} \right) + \frac{\partial}{\partial y} \left(\frac{h^3}{\mu} \frac{\partial P}{\partial y} \right) = 6u_x \frac{\partial h}{\partial x} + 6u_y \frac{\partial h}{\partial y} \quad (2)$$

设 $S = h/\mu^{1/3}$, $P = S^{-3/2} P'$, 则式(2)可变为如下的 Poisson 方程:

1992-11-13 收到初稿, 1993-03-18 收到修改稿。本文通讯联系人朱勤。

* 国家教委博士点基金资助项目。

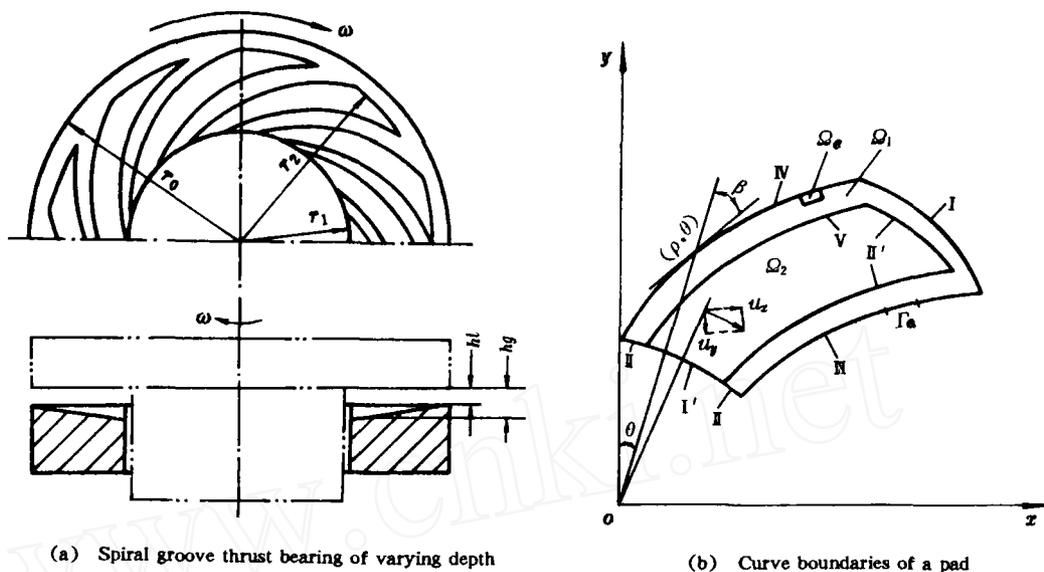


Fig. 1 Spiral groove thrust bearing of varying depth and curve boundaries of a pad

图 1 变深度螺旋槽止推轴承及单块瓦曲线边界

$$\begin{aligned} \nabla^2 P' &= \frac{\partial P'}{\partial r^2} + \frac{\partial^2 P'}{\partial \theta^2} \\ &= g_1 + g_2 P' = f(D) \end{aligned} \tag{3}$$

式中: D 为域内的点, 其基本解为 $P^*(C, D) = \ln[1/r(C, D)]$, $r(C, D)$ 为场点 C 到源点 D 的距离, 而

$$\begin{cases} g_1 = 6S^{-3/2} \frac{\partial h}{\partial \theta} \\ g_2 = \frac{3}{4} S^{-2} \left[\left(\frac{\partial S}{\partial r} \right)^2 + \left(\frac{1}{r} \frac{\partial S}{\partial \theta} \right)^2 \right] + \frac{3}{2} S^{-1} \left[\frac{1}{r} \frac{\partial}{\partial r} \left(r \frac{\partial S}{\partial r} \right) + \frac{1}{r^2} \frac{\partial^2 S}{\partial \theta^2} \right] \end{cases} \tag{4}$$

假设函数 u, v 在 $\Omega + \Gamma$ (Γ 为 Ω 的边界) 上具有二阶连续偏导数, 并取 $u = P', v = P^*$, 则由 Green 公式得到联系域内值 $P'(C), C \in \Omega$ 与边界值 $P'(D'), D' \in \Gamma$ 的关系式为:

$$\begin{aligned} P'(C) &= \frac{1}{2\pi} \int_{\Gamma} \left[\frac{\partial P'(D')}{\partial n(D')} P^*(C, D') - P'(D') \frac{\partial P^*(C, D')}{\partial n(D')} \right] d\Gamma(D') \\ &\quad + \frac{1}{2\pi} \int_{\Omega} f(D) P^*(C, D) d\Omega(D) \end{aligned} \tag{5}$$

若将域内点 C 取为边界上点 C' , 即 $C \rightarrow C', C' \in \Gamma$, 则可得边界积分方程:

$$\begin{aligned} C(C') P'(C') + \int_{\Gamma} P'(D) \frac{\partial P^*(C', D')}{\partial n(D')} d\Gamma(D') &= \int_{\Gamma} \frac{\partial P'(D)}{\partial n(D')} P^*(C', D') d\Gamma(D') \\ &\quad + \int_{\Omega} f(D) P^*(C', D) d\Omega(D) \end{aligned} \tag{6}$$

式中: $C(C')$ 是与 C' 点处边界几何形状有关的常数。

3. 边界积分方程的离散化及系数矩阵的解法

把边界 Γ 划分为 E_r 个边界线单元 Γ_e , 把区域 Ω 划分为 E_o 个四边形单元 Ω_e . 用 M_r 和 M_o

分别表示边界节点数和域内节点数,用 L_r 和 L_ω 分别表示 Γ_e 和 Ω_e 的节点数。

取线性边界单元,即 $L_r=2$,则在 Γ_e 上有:

$$P^l = \sum_{i=1}^{L_r} N_i^l P^{l,i}, \quad \frac{\partial P^l}{\partial n} = \sum_{i=1}^{L_r} N_i^l \left(\frac{\partial P^l}{\partial n} \right)^i \tag{7}$$

式中: $P^{l,i}$ 和 $(\partial P^l / \partial n)^i$ 分别为局部节点 i 的压力和外法线压力梯度, N_i^l 为对应于局部节点 i 的形状函数。

$$N_1^l = \frac{\xi_2 - \xi_1}{L_0}, \quad N_2^l = \frac{\xi - \xi_1}{L_0} \tag{8}$$

式中: ξ_1 和 ξ_2 分别为局部节点 $L_r=1,2$ 的坐标, L_0 为线单元 Γ_e 的长度,如图 2(a) 所示。

对域内单元 Ω_e 进行坐标变换,得:

$$x = \sum_{i=1}^{L_\omega} N_i^\omega x^i, \quad y = \sum_{i=1}^{L_\omega} N_i^\omega y^i \tag{9}$$

x^i 和 y^i 均为局部节点 i 的坐标, N_i^ω 为形状函数,当取双线性单元($L_\omega=4$)时有:

$$\begin{cases} N_1^\omega = \frac{1}{4}(1-\xi)(1-\eta), & N_2^\omega = \frac{1}{4}(1+\xi)(1-\eta) \\ N_3^\omega = \frac{1}{4}(1+\xi)(1+\eta), & N_4^\omega = \frac{1}{4}(1-\xi)(1+\eta) \end{cases} \tag{10}$$

把 Ω_e 变换为图 2(b) 所示的局部坐标系 $\xi\eta$ 下的标准单元,则在 Ω_e 上有:

$$f = \sum_{i=1}^{L_\omega} N_i^\omega f^i \tag{11}$$

在式(9)的坐标变换下有:

$$d\Omega = |J| d\xi d\eta \tag{12}$$

$$\begin{cases} |J| = \sqrt{E_0 G_0 - F_0^2}, & E_0 = \left(\frac{\partial x}{\partial \xi} \right)^2 + \left(\frac{\partial y}{\partial \xi} \right)^2 \\ G_0 = \left(\frac{\partial x}{\partial \eta} \right)^2 + \left(\frac{\partial y}{\partial \eta} \right)^2, & F_0 = \frac{\partial x}{\partial \xi} \frac{\partial x}{\partial \eta} + \frac{\partial y}{\partial \xi} \frac{\partial y}{\partial \eta} \end{cases} \tag{13}$$

对于边界 Γ 上的节点 n ,将式(9)和式(11)代入式(6),得:

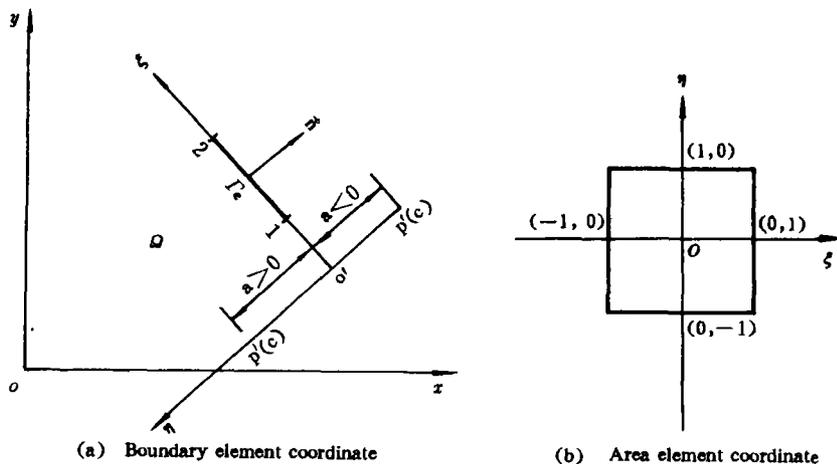


Fig. 2 Partial coordinate

图 2 局部坐标系

$$C^* P^{*'} + \sum_{\sigma=1}^{E_r} \int_{\Gamma_\sigma} \frac{\partial P^*}{\partial n} \sum_{l=1}^{L_r} P^{*'} N_l^l d\Gamma = \sum_{\sigma=1}^{E_r} \int_{\Gamma_\sigma} P^* \sum_{l=1}^{L_r} \left(\frac{\partial P^{*'}}{\partial n} \right)^l N_l^l d\Gamma + \sum_{\sigma=1}^{E_o} \int_{\Omega_\sigma} P^* \sum_{l=1}^{L_o} f^l N_l^o d\Omega \quad (14)$$

记为

$$C^* P^{*'} + \sum_{\sigma=1}^{E_r} \sum_{l=1}^{L_r} H_l^i P^{*'} = \sum_{\sigma=1}^{E_r} \sum_{l=1}^{L_r} G_l^i \left(\frac{\partial P^{*'}}{\partial n} \right)^l + \sum_{\sigma=1}^{E_o} \sum_{l=1}^{L_o} R_l^i f^l \quad (15)$$

式中:

$$H_l^i = \int_{\Gamma_\sigma} \frac{\partial P^*}{\partial n} N_l^l d\Gamma, \quad G_l^i = \int_{\Gamma_\sigma} P^* N_l^l d\Gamma, \quad R_l^i = \int_{\Omega_\sigma} P^* N_l^o d\Omega \quad (16)$$

式(15)可写成如下的矩阵形式:

$$[H]\{P\} = [G]\left\{\frac{\partial P}{\partial n}\right\} + [R]\{F\} \quad (17)$$

$$\begin{cases} H_{nm} = C^* \delta_{nm} + \sum_{\sigma=1}^{E_r} H_l^i & n, m = 1, 2, \dots, M_r \\ G_{nm} = \sum_{\sigma=1}^{E_r} G_l^i & n, m = 1, 2, \dots, M_r \\ R_{nm} = \sum_{\sigma=1}^{E_o} R_l^i & n = 1, 2, \dots, M_r \\ & m = 1, 2, \dots, M_r + M_o \end{cases} \quad (18)$$

H_{nm} 、 G_{nm} 和 R_{nm} 分别为矩阵 $[H]$ 、 $[G]$ 和 $[R]$ 中的元素。

对于域内 Ω 的节点 n , 式(5)同样可以离散成:

$$2\pi P^{*'} = [G]\left\{\frac{\partial P}{\partial n}\right\} - [H]\{P\} + [R]\{F\} \quad (19)$$

式中: $n = M_r + 1, M_r + 2, \dots, M_r + M_o$ 。

由图 2(a) 可知, $P^* = \ln \frac{1}{r} = -\frac{1}{2} \ln(\xi^2 + a^2)$, $\frac{\partial P^*}{\partial n} = -\frac{a}{\xi^2 + a^2}$, 则

$$\begin{cases} H_1^i = \int_{\Gamma_\sigma} N_1^l \frac{\partial P^*}{\partial n} d\Gamma \\ = \frac{\xi_2}{L_0} I_1 + \frac{1}{L_0} I_2 \\ H_2^i = \int_{\Gamma_\sigma} N_2^l \frac{\partial P^*}{\partial n} d\Gamma \\ = -\frac{1}{L_0} I_2 - \frac{\xi_1}{L_0} I_1 \end{cases} \quad (20)$$

$$\begin{cases} G_1^i = \int_{\Gamma_\sigma} N_1^l P^* d\Gamma \\ = \frac{\xi_2}{L_0} I_3 + \frac{1}{L_0} I_4 \\ G_2^i = \int_{\Gamma_\sigma} N_2^l P^* d\Gamma \\ = -\frac{1}{L_0} I_4 - \frac{\xi_1}{L_0} I_3 \end{cases} \quad (21)$$

式中:

$$\begin{cases}
 I_1 = \begin{cases} - \left[\operatorname{tg}^{-1} \frac{\xi}{a} \right]_{\xi_1}^{\xi_2} & a \neq 0 \\ 0 & a = 0 \end{cases} \\
 I_2 = \begin{cases} \left[\frac{a}{2} \ln(\xi^2 + a^2) \right]_{\xi_1}^{\xi_2} & a \neq 0 \\ 0 & a = 0 \end{cases} \\
 I_3 = \begin{cases} \left[\xi - \frac{\xi}{2} \ln(\xi^2 + a^2) \right]_{\xi_1}^{\xi_2} & a \neq 0 \\ 0 & a = 0 \end{cases} \\
 I_4 = \begin{cases} \frac{1}{4} [(\xi^2 + a^2) \ln(\xi^2 + a^2) - \xi^2]_{\xi_1}^{\xi_2} & a \neq 0 \\ 0 & a = 0 \end{cases}
 \end{cases} \quad (22)$$

设局部节点 1、2 的坐标分别为 (x^1, y^1) 和 (x^2, y^2) , 场点 C 的坐标为 (x^*, y^*) , O' 点的坐标为 (x^0, y^0) , 则

$$\begin{cases}
 a = -(x^* - x^0) \sin \varphi + (y^* - y^0) \cos \varphi \\
 \xi_1 = (x^1 - x^0) \cos \varphi + (y^1 - y^0) \sin \varphi \\
 \xi_2 = (x^2 - x^0) \cos \varphi + (y^2 - y^0) \sin \varphi \\
 \operatorname{tg} \varphi = \frac{y^2 - y^1}{x^2 - x^1}
 \end{cases} \quad (23)$$

R_i^* 的积分在图 2(b) 所示的标准单元上完成, 得:

$$\begin{aligned}
 R_i^* &= \int_{\omega_e} P^* N_i^* d\Omega \\
 &= \int_{-1}^1 \int_{-1}^1 P^* N_i^* |J| d\xi d\eta \\
 &= \sum_{i=1}^6 \sum_{j=1}^6 \omega_i \omega_j (P^* N_i^* |J|)_{\xi_i, \eta_j}
 \end{aligned} \quad (24)$$

式中: ω_i 和 ω_j 都是 Gauss 积分权系数, ξ_i 和 η_j 均为 Gauss 积分点坐标, $(\cdot)_{\xi_i, \eta_j}$ 表示括号内的函数取 ξ_i 和 η_j 处的值。

关于角点系数 C^n 的求法是假设在所研究的区域内存在一等压无源压力场, 即 $\left\{ \frac{\partial P}{\partial n} \right\} \equiv 0$, $\{F\} \equiv 0$, 则由式(17)可得:

$$H_{nm} = - \sum_{\substack{m=1 \\ m \neq n}}^{M_r} H_{nm} \quad (25)$$

从而避免了角点系数的计算。

4. 变深度螺旋槽止推轴承的边界条件

如图 1(b) 所示, 对于区域 Ω_1 , 设其各条边界上的压力值分别为 P_I 、 P_{II} 、 P_{III} 、 P_{IV} 和 P_V , 而且 $f=0$; 对于区域 Ω_2 , 设其各条边界上的压力值分别为 $P_{I'}$ 和 $P_{II'}$, 则每条边界应用式(17)可得一个方程, 共计 7 个方程 14 个变量, 其定解条件为:

a. 边界 I 和边界 II、I' 分别为出油边和进油边, 其压力值为:

$$\begin{cases} P_I = 0 \\ P_{I'} = P_{II'} = P_{III} = \text{常数} \end{cases} \quad (26)$$

b. 边界 III 和 IV 满足周期性条件, 即

$$\begin{cases} P_{III} = P_{IV} \\ \frac{\partial P_{III}}{\partial n} = -\frac{\partial P_{IV}}{\partial n} \end{cases} \quad (27)$$

c. 边界 V 和 II' 为同一条公共边界, 应满足压力值相等和流量连续的条件:

$$\begin{cases} P_V = P_{II'} \\ \frac{\omega r h_i}{2} \cos(\vec{n}, \vec{v}) - \frac{h_i^3}{12\mu} \frac{\partial P_V}{\partial n} = - \left[\frac{\omega r h_g^3}{2} \cos(\vec{n}, \vec{v}) - \frac{h_g^3}{12\mu} \frac{\partial P_{II'}}{\partial n} \right] \end{cases} \quad (28)$$

5. 变深度螺旋槽止推轴承性能的计算

令 $B = r_2 - r_1$, $h = h_m H$, $\mu = \mu_0 \bar{\mu}$, $P = \mu_0 \omega B^2 \bar{P} / h_m^2$, $R = r/B$, $\rho = BR$, 则螺旋槽曲线的无量纲形式为:

$$R = R_1 e^{i\theta} \quad (29)$$

而单块瓦的无量纲承载力、进油量和摩擦力矩分别为:

$$\bar{W} = \frac{W}{\mu_0 \omega B^4} = \iint \bar{P} R d\theta dR \quad (30)$$

$$\bar{Q}_{in} = \frac{Q_{in}}{\omega B^2 h_m} = - \int \frac{H^3}{12\mu} \frac{\partial \bar{P}}{\partial R} R d\theta \quad (31)$$

$$\bar{M}_t = \frac{M}{\mu_0 \omega B^4} = \iint \left(\frac{\bar{\mu} R^2}{H} + \frac{H}{2} \frac{\partial \bar{P}}{\partial \theta} \right) R d\theta dR \quad (32)$$

当取变深度螺旋槽止推轴承的无量纲尺寸为 $R_1 = \frac{r_1}{B} = 1.4$, $R_2 = \frac{r_2}{B} = 2.4$, $R_0 = \frac{r_0}{B} = 2.5$

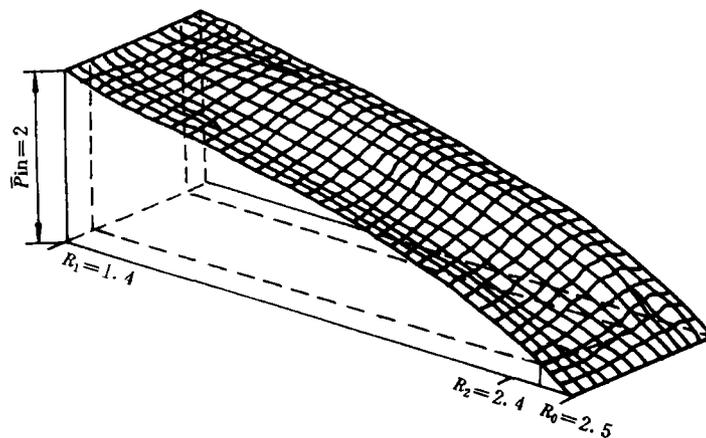


Fig. 3 Dimensionless pressure distribution of a pad in the bearing

图 3 轴承中单块瓦的无量纲压力分布

时,轴承中单块瓦的无量纲压力分布见图3所示,其承载力、进油量和摩擦力矩等性能参数见表1所列。

表1 轴承中单块瓦的无量纲承载力、进油量和摩擦力矩等性能参数

Table 1 Dimensionless load carrying capacity, input oil flow rate and frictional torque of a pad in the bearing

β	$H_i=1, H_g=-2.5R+7, \bar{P}_{in}=1$			$H_i=1, H_g=-2.5R+7, \bar{P}_{in}=2$			$H_i=1, H_g=-5R+13, \bar{P}_{in}=1$			$H_i=1, H_g=-5R+7, \bar{P}_{in}=2$		
	\bar{W}	\bar{Q}_{in}	\bar{M}_t	\bar{W}	\bar{Q}_{in}	\bar{M}_t	\bar{W}	\bar{Q}_{in}	\bar{M}_t	\bar{W}	\bar{Q}_{in}	\bar{M}_t
70°	1.309	1.584	4.724	2.476	2.588	5.014	1.196	0.574	4.562	2.310	0.949	4.179
60°	1.334	1.568	4.952	2.533	2.473	5.431	1.219	0.569	4.604	2.356	0.898	4.311
50°	1.384	1.534	5.257	2.642	2.350	5.982	1.260	0.563	4.717	2.442	0.855	4.498

6. 结 论

- 本文为变深度螺旋槽止推轴承性能的计算提供了一种有效的方法——边界元法。
- 随着螺旋角 β 的减小,承载力 \bar{W} 和摩擦力矩 \bar{M}_t 都增大,但进油量 \bar{Q}_{in} 减小。
- 当 H_i 由 $-2.5R+7$ 变为 $-5.0R+13$ 时,承载力 \bar{W} 、进油量 \bar{Q}_{in} 和摩擦力矩 \bar{M}_t 都减小。
- 供油压力 \bar{P}_{in} 越高,承载力 \bar{W} 和进油量 \bar{Q}_{in} 都越大,而摩擦力矩 \bar{M}_t 的变化却取决于 H_g 。当 $H_g=-2.5R+7$ 时, \bar{M}_t 增大,但当 $H_g=-5.0R+13$ 时, \bar{M}_t 却减小。

参 考 文 献

- [1] Smalley, A. J., "The Narrow Groove Theory of Spiral Groove Gas Bearing: Development and Application of a Generalized Formulation for Numerical Solution", Journal of Lubrication Technology, Trans. ASME, Jan. 1972, p. 86-92.
- [2] Gupta, P. K. et al., "Ambient Edge Correction for the Locally Incompressible Narrow-Groove Theory", Journal of Lubrication Technology, Trans. ASME, Apr. 1974, p. 284-290.
- [3] Murata, S. et al., "On a Two-Dimensional Theory of Spiral Groove Bearing", Proc. JSLE-ASLE, Intern. Lubr. Conf., 1975, p. 237-245.
- [4] 朱勤, 谢友柏, 虞烈, 薛永宽, 摩擦学学报, 13(1993)17.
- [5] Muijderman, E. A., "Spiral Groove Bearing", Printed in the Netherlands, 1966, Preface.
- [6] Hing, F. C., "Analytical Solution for Incompressible Spiral Groove Viscous Pumps", Journal of Lubrication Technology, Trans. ASME, July 1974, p. 365-369.
- [7] Murata, S. et al., "Exact Two-Dimensional Analysis of Circular Disk Spiral Groove Bearing", Journal of Lubrication Technology, Trans. ASME, Oct. 1979, p. 424-436.
- [8] Murata, S. et al., "Exact Two-Dimensional Theory of Spherical Spiral Groove Bearings", Journal of Lubrication Technology, Trans. ASME, Oct. 1980, p. 430-438.
- [9] 王元淳, 边界元法基础, 上海交通大学出版社, 上海, 1988, p. 3.

Calculation of a Spiral Groove Thrust Bearing of Varying Depth with Boundary Element Method

Zhu Qin Xie Youbai Yu Lie Xue Yongkuan

(Theory of Lubrication and Bearing Institute,
Xi'an Jiaotong University, Xi'an 710049, China)

Abstract As the pressure control equation (i. e. Reynold's Equation) was transformed into Poisson's Equation in this paper, the pressure distribution is solved using Boundary Element Method. The step numbers of algebraic equation group are effectively dropped, the calculation time of computer is largely decreased and the precision of calculation result is raised. Because spiral groove bearings are of higher load-carrying capacity and less friction force in comparison with the other bearings under high speed condition, they are widely used in high speed rotating machinery. Therefore, a spiral groove thrust bearing of varying depth is choosed as an example of the application of Boundary Element Method in the paper. The treatment of boundary condition is introduced and the influence of dimensional parameters on bearing's performance, such as load-carrying capacity, flow rate and frictional torque are discussed. Also, satisfactory results are presented.

Key words spiral groove, thrust bearing, Boundary Element Method, mechanics of lubrication